The 7th International Supercritical CO_2 Power Cycles Symposium
March 31 – April 2, 2020, San Antonio, Texas
Paper # 082

Investigation of Recompression Supercrtical CO2 cycle

Jarosław Milewski
Warsaw University of Technology
Warsaw, Poland

Piotr Lis
Warsaw University of Technology
Warsaw, Poland

Łukasz Szabłowski
Warsaw University of Technology
Warsaw, Poland

Arkadiusz Szczęśniak
Warsaw University of Technology
Warsaw, Poland

Olaf Dybiński
Warsaw University of Technology
Warsaw, Poland

Marcin Wołowicz
Warsaw University of Technology
Warsaw, Poland

ABSTRACT

The paper contains off-design simulations of super critical CO2 recompression cycle with various system control strategies. The closed cycle is controlled by varying the bypass valve of the main compressor and turbine inlet temperature to achieve the target system power and rotational shaft speed. Performance maps were generated based on the off-design simulation. The maps can be used to estimate the control parameters dependencies and develop an efficient system controller. Other more complex strategies not considered in this study may also be used, such as turbine wastegate or compressor inlet pressure and temperature control.

INTRODUCTION

Energy needs have grown in recent decades due to economic and population growth. The heavy use of fossil fuels has led to concerns in respect of greenhouse gas emissions (Sadeghi 2019). It is widely accepted that new solutions for clean and sustainable energy are becoming a critical factor for the future of society (Leonzio 2018). Many researchers predict that in future the energy market will be based on hydrogen as primary energy carrier. Water electrolysis (Amaral 2018, Barelli 2018, Guo 2019, Xing 2018) is certainly the cleanest method for hydrogen production and it is seen as the energy vector of a truly green and efficient energy system, if the electricity used in the process comes from renewable sources. Touted as the most favorable future scenario are: large scale use of renewable energy (Clúa 2018) and/or biofuels (Recalde 2018). In the short term, one measure that can be taken here is to utilize waste energy. Renewable energies such as solar and wind are by nature intermittent, as they are dependent on weather conditions (Perez-Trujillo 2018). Thus, the use of waste heat is a very attractive topic in many areas of power engineering. Usually, it can be done by coupling the waste generating system with closed-cycle externally-heated bottoming systems, and there are a few options to suit different output ranges (Ye 2018, Roy 2019). In some cases the gas turbine cycle can be include directly in the host system, opening the way to regulation of the host system through controlling a compressor inlet flow (guide vane) (Boroumand 2019, Lv 2018) and to reduced exergy losses

of the combustor (by using a fuel cell to substitute for this unit) (Marefati 2019, Badur 2018). Supercritical carbon dioxide at 800°C can be used for a high temperature Brayton cycle, which has the potential to achieve a more compact power cycle with higher efficiency than the steam Rankine cycle (Chen 2018).

(Sánchez 2011) presents an assessment on the expected part load performance of the Molten Carbonate Fuel Cell -- supercritical Brayton cycle hybrid system, where a simple recuperative carbon dioxide cycle was considered instead of the more complicated recompression cycle. Various control strategies for part load operation were considered and incorporated: inventory control, by-pass control and temperature control. Performance analysis of the bottoming system under similar part load operating conditions at the fuel cell was carried out. The results show that the proposed system had excellent part load performance and, more specifically, the benefit of mixed control instead of using a single technique, which is not feasible in practice due to operational limits (see Fig. 1).

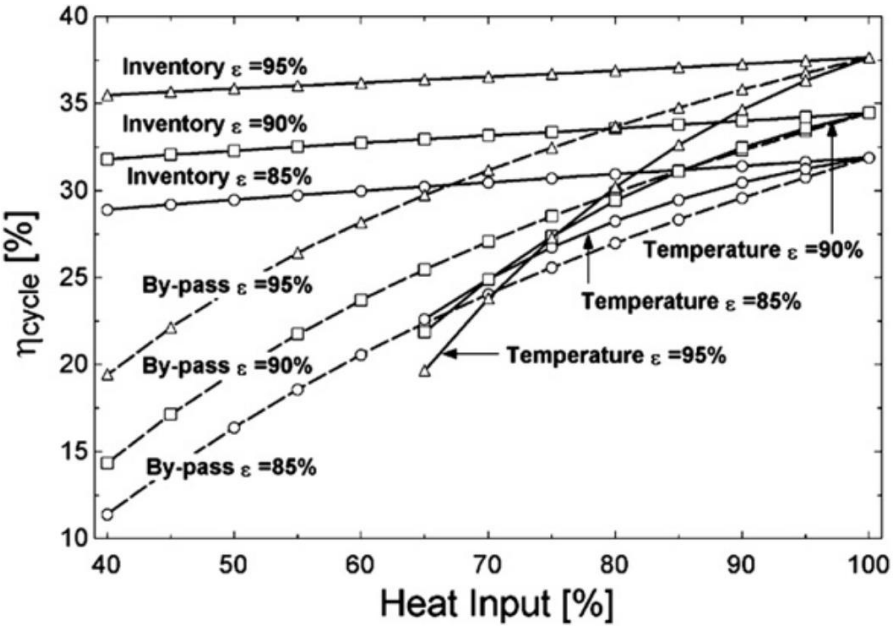

Fig. 1 Cycle performance for different heat exchanger effectiveness (Sánchez 2011)

Research findings (Dyreby 2011) suggest that the optimal design for turbomachinery in a supercritical carbon dioxide (S-CO2) Brayton power cycle, considering its overall performance, may not coincide with the optimal design suggested by simple on-design thermodynamic analysis. Initial results suggest that designing for a higher compressor inlet temperature will not significantly degrade plant efficiency and it may yield better off-design power production, possibly increasing overall power plant performance as evaluated on an annual basis. These results are particularly relevant to renewable energy applications that are inherently transient, such as concentrating solar power (CSP) systems. Research by the same people two years later (Dyreby 2013) highlighted the importance of actively controlling the low-side pressure in order to optimize thermal efficiency, while ongoing work focuses on modeling off-design performance of the cycle on an annual basis (see Fig. 2). Particularly interesting is the effect of design point low side temperature selection on the annual performance of the cycle. A discussion of modeling and control issues is presented in a subsequent paper (Dyreby 2014).

Startup, shutdown, and off-design operation of a supercritical carbon dioxide (sCO2) based Recompression Brayton Cycle (RCBC) powered using an oxygen fired coal pressurized fluidized bed combustor (PFBC) were studied in (Vega 2014). In fact, there is a dynamic response presented in the paper, but no off-design characteristic included directly.

(Louis 2016) investigates optimal design and operation of supercritical carbon dioxide power cycles for concentrating solar power applications. Previous design-point and off-design studies have supported potential efficiency improvements and established broad operating conditions for the supercritical carbon dioxide power cycle at temperatures pertinent to concentrating solar power applications. They investigate a simple/recompression supercritical carbon dioxide cycle integrated with molten salt heat source and maximized cycle efficiency for off-design operation. The findings of this study report optimal operating parameters under off-design conditions and provide an understanding of the effect of cycle parameters on other primary subsystems in a concentrating solar power plant.

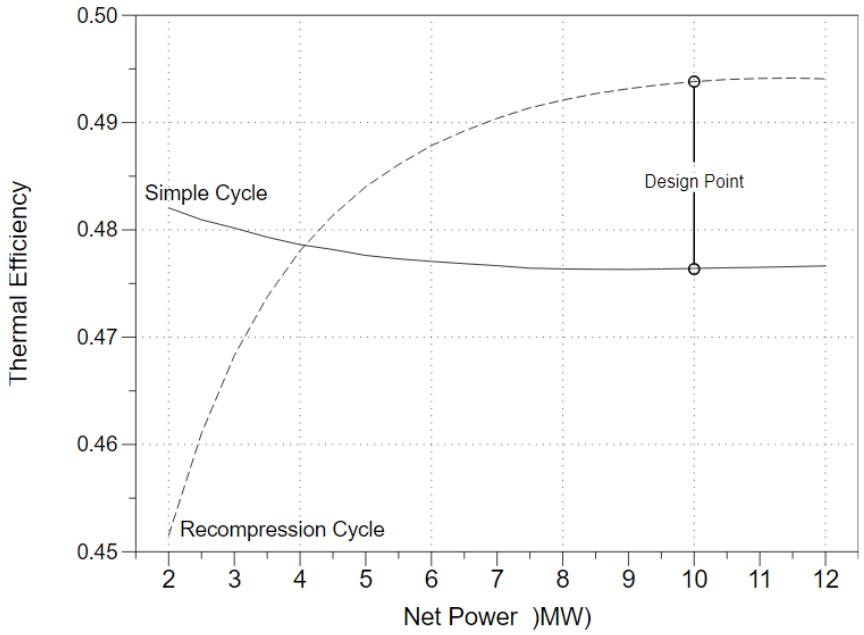

Fig. 2 Optimal part-load efficiency of the simple (solid line) and recompression (dashed line) Brayton cycles (Dyreby 2013)

(Hoopes 2016) discusses the development of a tool to evaluate off-design heat exchanger performance without specifying heat exchanger geometry. Special attention is given to the application of this tool to heat exchangers found in supercritical carbon dioxide power cycles.

The optimum control strategies obtained by repetitive quasi-steady state analyses under various off-design conditions were investigated in (Kwon 2018), based on the developed off-design model. The bulk of the effort was put into modifying the calculation algorithm of a heat exchanger.

The results of off-design performance models for a supercritical CO2 (sCO2) waste heat recovery power cycle is presented in (Wright)---see Fig. 4. The paper discusses the primary control mechanisms, which include (1) varying the air-cooling fan speed, by (2) changing the boost compressor speed, by (3) varying the split-flow fraction, by (4) selecting the compressor

inlet pressure. Examples of the system response to these control variables were discussed using plots and curves that showed the net power and the state-point temperatures (see Fig. 5). The report then demonstrates that the combination of the four control mechanisms provides an effective means to mitigate the effects of increases in ambient heat rejection temperature.

The turbine part of the supercritical CO2 cycle was analyzed in (Zhang 2018), where three types of nozzle profiles were taken into account.

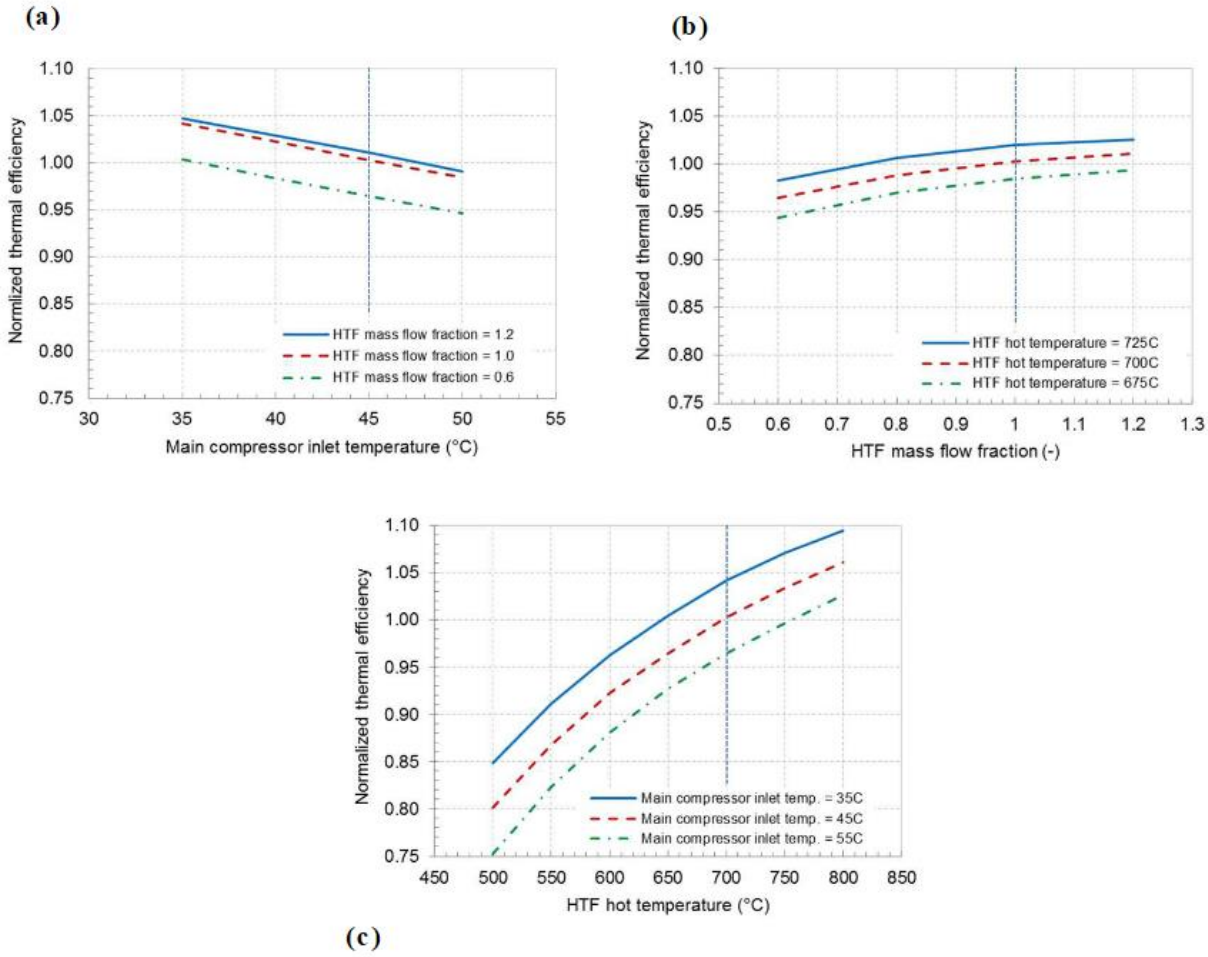

Fig. 3 Design of experiments study of various off-design conditions, investigating the main and interaction effects: a) main compressor inlet temperature, b) mass flow fraction, and c) HTF hot temperature. Design-point values are given by the dashed vertical line (Louis 2016)

A summary of the literature review is presented in Table 1, where the ranges of investigated parameters are indicated according to the dependent variables used for cycle characteristics. The most important parameter is cycle thermal efficiency, investigated from various angles.

Our previous work indicates that the most effective cycle based on carbon dioxide at super critical state is a Recompression Brayton (see Fig. 7). This concept, based on two compressors

in the cycle can be found in other systems like Graz cycle (Juangsa 2018). The cycle was created in Eblison, commercially available software. The results based on design point calculations are very promising and detailed calculation tools were deemed essential for component design and off-design analysis (Ferrari 2018). Here, we explore the system, indicating the possible operation ranges of the system. To do so requires scaling the elements of the system and implementing the off-design characteristics. Various works indicate different power ranges of such systems, depending on the proposed application.

Solar power and waste heat can be varied in the range 1 ... 40 MW for solar tower, through 2 MW_{th} for solar assisted systems, 9 MW for parabolic collector array, 7 .. 22 MW when used in solar heliostat applications (Wang 2017, Luu 2017, Luu 2018, Milani 2017, Wang 2018, Reyes-Belmonte 2016, Passos 2018, Atif 2017). Waste heat can be recovered by recompression super critical CO2 based Brayton cycle with power range 2 MW_{th} .. 270 MW (Banik 2016, Hou 2017, Calle 2018, Wang 2016). Classical systems equipped with a steam turbine for ORC application are predicted to be in the range of 48 .. 262 MW (Hou 2018) . The largest applications are classified for nuclear power (including helium reactors) in the power range of 41.5 .. 1,500 MW (Al-Sulaiman 2016, Deng 2017, Wu 2017, Wu 2018, Jeong 2011, Akbari 2014, Floyd 2013, Dyreby 2014). Additionally, in the available literature, the system can be coupled with other cycles (e.g. steam (Hou 2018)).

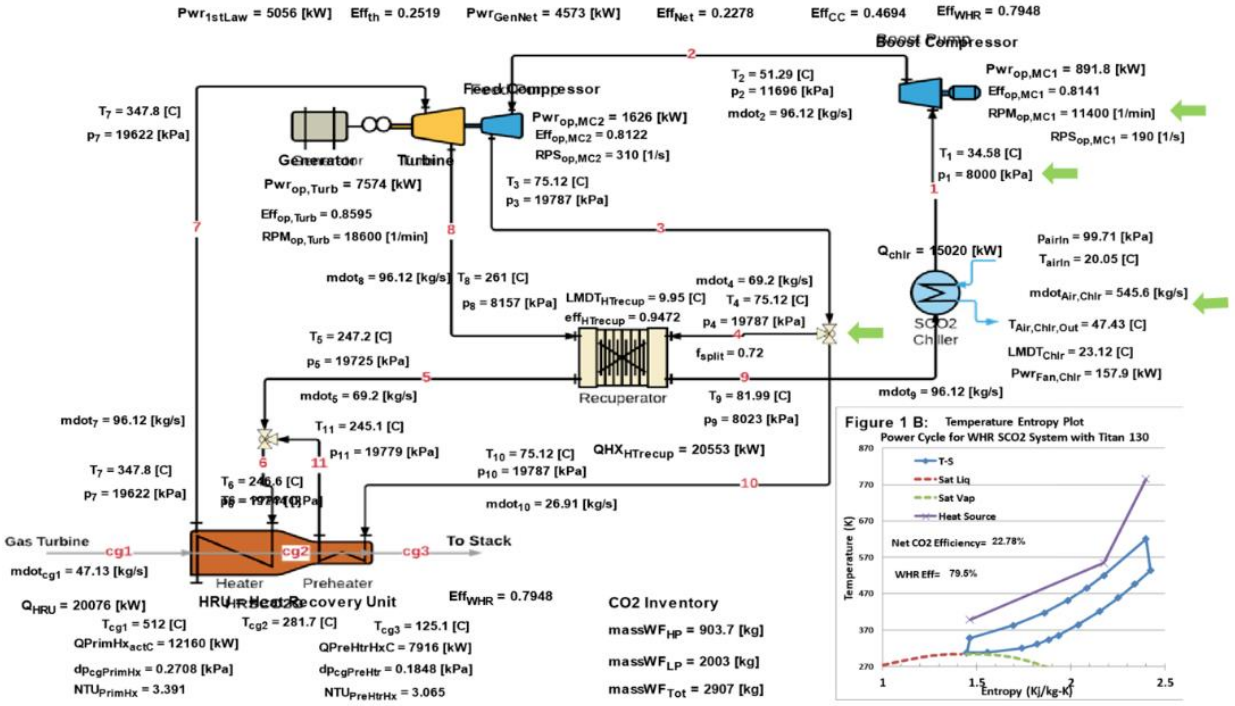

Fig. 4 Process flow diagram for the 5 MW_e sCO2 Waste Heat Recovery Power Plant (Wright)

Thus, the choice is not obvious here what size of plant and sizes of equipment should be chosen for further investigation. Fortunately, the most advanced studies in the topic are based on a real demonstration plant proposed by the company Sandia. Some details can be found in a paper which describes control of a Supercritical CO2 Recompression Brayton Cycle Demonstration Loop, as presented in (Conboy 2013), based on the Sandia recompression Brayton cycle facility which was designed and built as an S-CO2 power cycle demonstration. At around 1 MW_{th} in

size, the loop was intended to be large enough to confront the fundamental issues for this technology, but small enough to be affordable over several years at the maximum funding expected within DOE research budgets.

Then we will finally focus on the 1 MW_{th} demonstration plant for which the most data are already known and published. We will explore the off-design operation of the plant with some critical regimes of operational ranges.

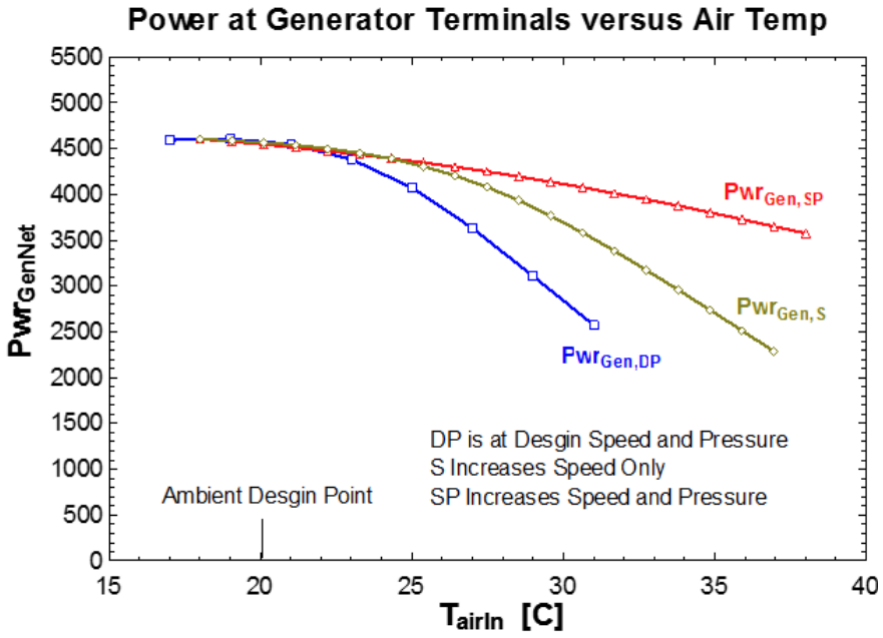

Fig. 5 Example illustrating the performance of the sCO2 power plant as a function of ambient inlet air temperature for design point operating conditions (DP; blue curve). The 2nd case (green curve) increases the MC1 shaft speed from 11400 to 16800 rpm and with increasing air-cooling fan speed (and with minor split flow fraction changes). The 3rd case also increases compressor inlet pressure (Wright)

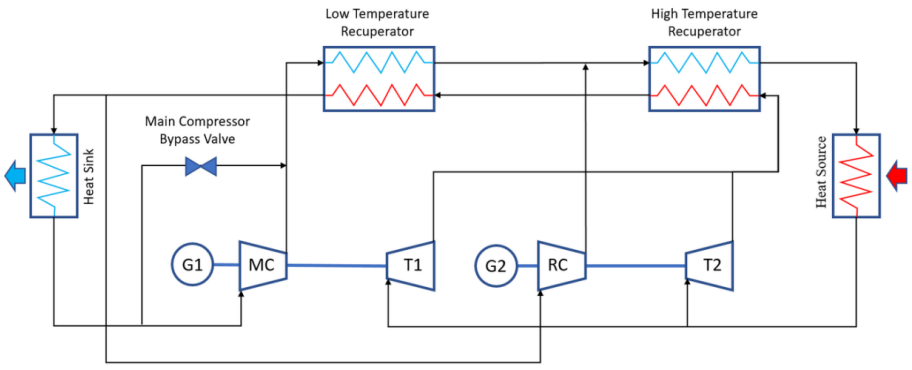

Fig. 6 Schematic diagram of the recompression Brayton cycle with main compressor bypass valve

RESULTS AND DISCUSSION

The system is modeled in off-design mode using Ebsilon, commercially available software. Previously, we built separate models of each element of the system.

There are two ways of developing mathematical models. They can be developed as analytical models on the basis of laws of conservation or as empirical models on the basis of measured data (Plis 2018). A mathematical model of the gas turbine unit includes partial models of a compressor, heat exchanger and an expander. The partial model of the compressor was built up with a compressor map, which describes the relationship between the corrected air mass flow rate, the pressure ratio and the corrected rotational speed. The partial model of the expander contains a flow capacity equation and an equation for the internal efficiency of the expander. The unknown values of the empirical coefficients, which appear in these equations, can be estimated on the basis of measured data results.

Table 1: Summary of literature review

Indepedent variable	Dependent variable	Range	Comments
Heat input, %	Cycle efficiency,%	40 .. 100	\cite{S_nchez_2011}
Net power, %	Thermal efficiency, %	17 .. 100	\cite{Dyreby_2013}
Main compressor inlet temperature, °C	Thermal efficiency, %	35 .. 50	\cite{louis2016analysis}
Heat transfer fluid mass flow ratio	Thermal efficiency, %	60 .. 120	\cite{louis2016analysis}
Heat transfer fluid hot temperature, °C	Thermal efficiency, %	500 .. 800	\cite{louis2016analysis}
Ambient air temperature, °C	Power, kW	15 .. 40	(Wright et al.)

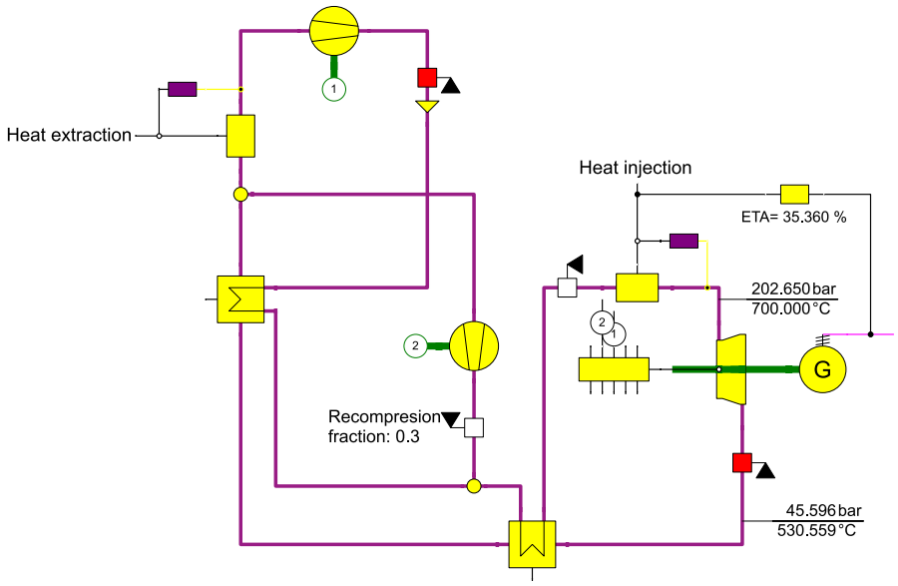

Fig. 7 Schematic diagram of the recompression Brayton cycle implemented in Ebsilon software

Controlling a closed cycle is no trivial issue. There are a few ways to do this, e.g. by storing part of the working fluid in an additional pressurized tank, but the cheapest solution is by using a by-pass. During dynamic changes we need to control several variables by control loops (Botta 2019, Ma 2018, S. 2018); fuzzy logic control systems (Siddiqui 2018) and artificial neural networks (Xia 2018) can be applied, but this issue falls outside the remit of this work.

Compressor

Compressor performance during off-design operation was calculated through the use of a map. On the base of provided experimental data, GT-POWER software creates a map that is interpolated between the given data points and extrapolated to a pressure ratio of 1.0 and speed of 0.0 RPM. Raw data (suction and discharge temperature/pressure) are directly entered and then corrected during preprocessing from actual speed to corrected speed. For each point, the following data are used: corrected speed, corrected mass flow rate, pressure ratio and efficiency. GT-POWER does not require the pressure ratio to be static outlet divided by total inlet. The RMP is corrected due to the temperature:

$$RPM_{corrected} = RPM_{actual} / \sqrt{\frac{T_{in\ total}}{298}}$$

The mass flow rate is corrected due to the temperature and pressure:

$$\dot{m}_{corrected} = \dot{m}_{actual} \sqrt{\frac{T_{in\ total}}{298}} / \frac{P_{in\ total}}{100}$$

The pressure ratio is made the following way:

$$PR_{scaled} = 1.0 + PR_{multiplier}(R_{original} - 1.0)$$

Turbine

The turbine model in question is reduced to a model of the turbine stage group. Two essential characteristics are needed: flow capacity and efficiency changes under variable operating conditions.

The first step in building the model is adapting the turbine map provided by the manufacturer. This adaptation consists in creating a reduced map (to adapt it for other inlet conditions) and interpolation of curves between points as well as extrapolation for the edge of the map for low speeds and low pressures.

The input data is divided into two groups: reduced mass flow and efficiency. The group with reduced flow will consist of a set of work points defined by: corrected speed, pressure ratio and reduced mass flow. The efficiency group will consist of a set of work points defined by: corrected speed, pressure ratio and efficiency. The same speed curves must exist in both groups. The speed curves in the two groups need not have the same pressure ratio. The tool used for modeling (GT-SUITE) will unify both versions of the speed curves into a single speed curve.

The rotational speed should be corrected due to the temperature:

$$RPM_{corrected} = RPM_{actual}\sqrt{\frac{T_{ref}}{T_{in\ total}}}$$

If the measurement data for the turbine map was collected on another working medium, this should be taken into consideration when correcting the speed:

$$RPM_{corrected} = RPM_{actual}\sqrt{\left(\frac{\gamma_{ref}}{\gamma_{act}}\right)\left(\frac{R_{ref}}{R_{act}}\right)\left(\frac{T_{ref}}{T_{in\ total}}\right)}$$

where: R-Individual gas constant, γ-specific heats ratio.

To build a turbine map a reduced mass flow rate is needed:

$$\dot{m}_{reduced} = \frac{\dot{m}_{actual}\sqrt{T_{in\ total}}}{P_{in\ total}}$$

where: p–is pressure.

To improve the accuracy of the simulation due to the changes in the ratio of specific heat (γ) and the individual gas constant (R), a reduced mass flow rate can be described by the following equation:

$$\dot{m}_{reduced} = \frac{\dot{m}_{actual}\sqrt{T_{in\ total}}}{P_{in\ total}}\sqrt{\left(\frac{\gamma_{ref}}{\gamma_{act}}\right)\left(\frac{R_{ref}}{R_{act}}\right)}$$

Heat Exchanger

The heat exchanger model describes the geometry, heat transfer performance data and pressure drop for the heated and cooled fluid. Geometry is defined using the reference object where heat transfer performance between the fluid and the wall of heat exchanger are described by entering measured data of the heat exchanger geometry and reference length for the Reynolds Number. The software calculates the Nusselt correlations during pre-processing of the simulation. Minimum Nusselt Numbers can be defined if required to keep the value within a specified boundary. Pressure drop, in order to be defined most accurately, is also presented as a reference object. This allows the heat exchanger to be scaled for various operating points.

Temperature is evaluated for all thermal properties of fluid (viscosity, specified heat, conductivity) at a specified point, meaning that the actual temperature difference between fluid and wall can be determined. It is calculated as a weighted value on the inlet and outlet temperature of the pipe:

$$T_{fluid} = cT_{out} + (1 - c)T_{in}$$

where c - distance from the beginning of the pipe. For example, the fluid temperature used for the fluid properties lookup on the outlet of the pipe uses c=1, while average temperature assumes c=0.5.

Heat transfer correlations are calculated separately for heating and cooling cases.

For Single Phase Liquid, Single Phase Vapor and for Single Phase Supercritical, the Dittus-Boelter correlation is used:

Heating:

$$h = 0.023 * Re^{0.8} * \mathrm{Pr}^{0.4} \frac{k}{D}$$

Cooling:

$$h = 0.023 * Re^{0.8} * \mathrm{Pr}^{0.3} \frac{k}{D}$$

and this is valid for fully developed flow (L/D >=10) 0.7<=Pr<=160, Re>=10,000

For Two Phase Condensation and Two-Phase Evaporation tube correlation is used (Shah 1979), which is a tube-style heat transfer correlation appropriate for film-type condensation in round tubes. The flow is assumed to be annular with uniform film distribution. The correlation applies to both horizontal and vertical tubes:

$$Nu_t = 0.023 * Re^{0.8} * \mathrm{Pr}^{0.4}$$

$$h = Nu_t \left((1-x)^{0.8} + \frac{3.8 * x^{0.76} (1-x)^{0.04}}{Pr^{0.38}} \right) \frac{k}{D}$$

And this is valid for 0.002<Pr<0.44, 0<x<1, 10.8 kg/(m2*s)<G<1599 kg/(m2*s)

Off-design operation of the recompression super critical CO2 cycle

Using the off-design simulation model, different supercritical CO2 cycle control strategies were investigated. The analyzed system contained two compressor-turbine-generator units, high and low temperature recuperator, heat source and heat sink, as shown on Fig. 6. Rotational speed, turbine inlet temperature (TIT) and main compressor bypass valve opening were used as parameters in the design of the experimental study. The following TIT range was considered: 500 .. 1200 K. The following reduced rotational speed range was considered: 3436 .. 5153 rpm.

The system characteristics are presented on a pressure ratio vs reduced mass flow map of performance. On the maps, the vertical lines represent the turbine inlet temperature, whereas horizontal lines represent reduced rotational speed of the shaft, total system efficiency is also presented as separated curves. Map can be used to develop system control strategy for different operating conditions, using the main compressor bypass valve.

Three different performance maps were created, each map for different main compressor bypass valve positions:

I - fully closed,

II - partially open,

III - fully open.

The following relative valve cross section area corresponds to each position:

I - 0%,

II -25%,

III - 100%.

The valve operating range was limited to avoid close-to-zero system efficiencies resulting from non-optimal main compressor performance.

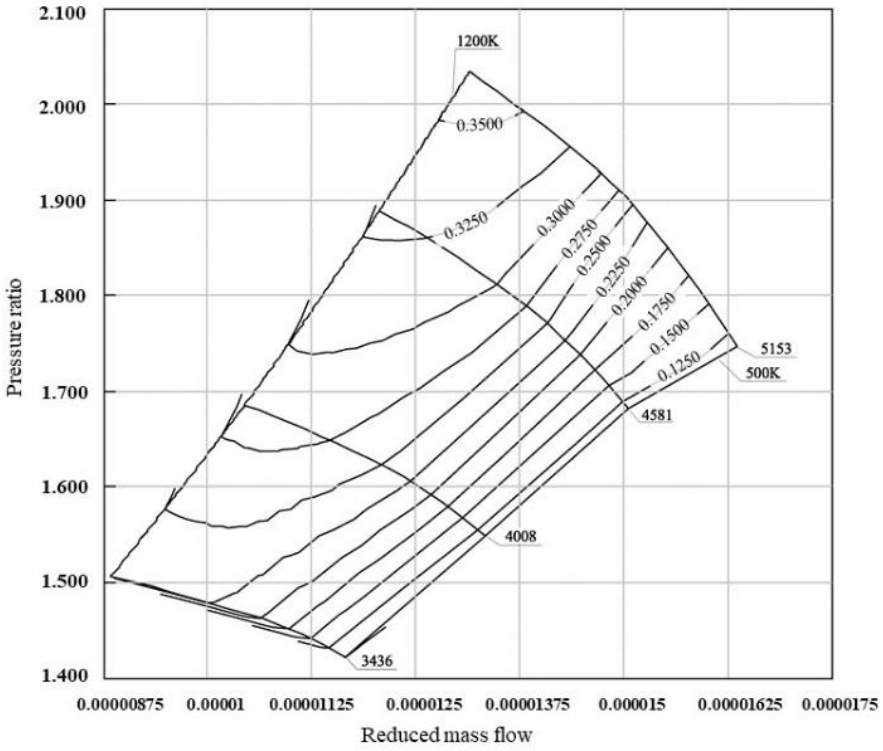

Fig. 8 Performance map, main compressor bypass valve 0% open

Fig. 8 shows a system performance map when the main compressor valve is fully closed. This represents normal system operation. System efficiency varies from 13 to 35% within the operation range and peaks at highest TIT and highest rotational speed.

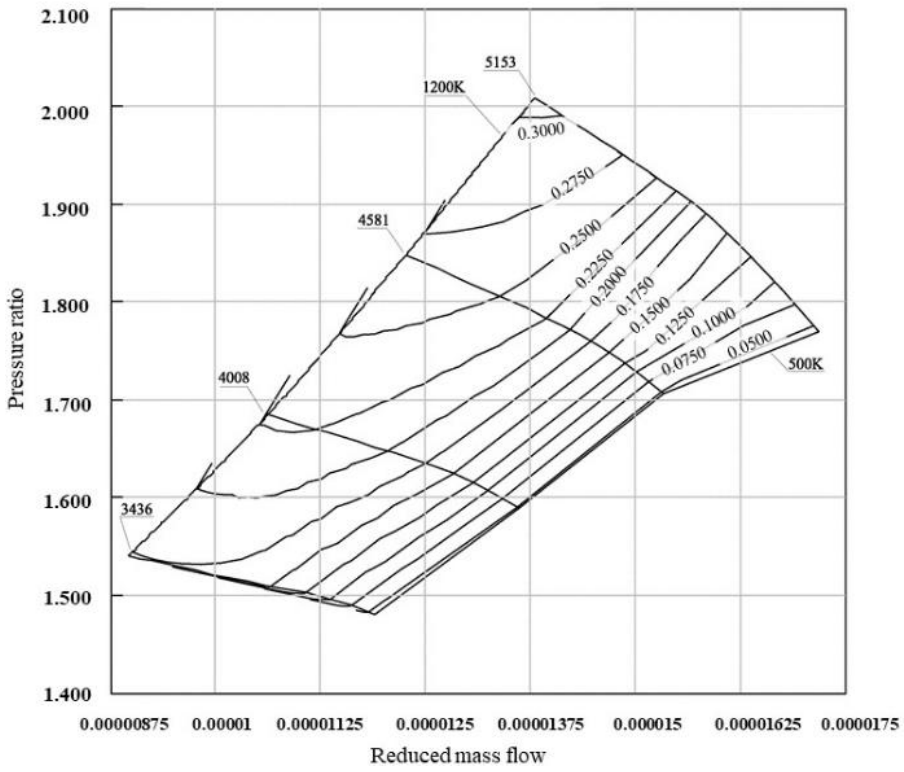

Fig. 9 Performance map, main compressor bypass valve 25% open

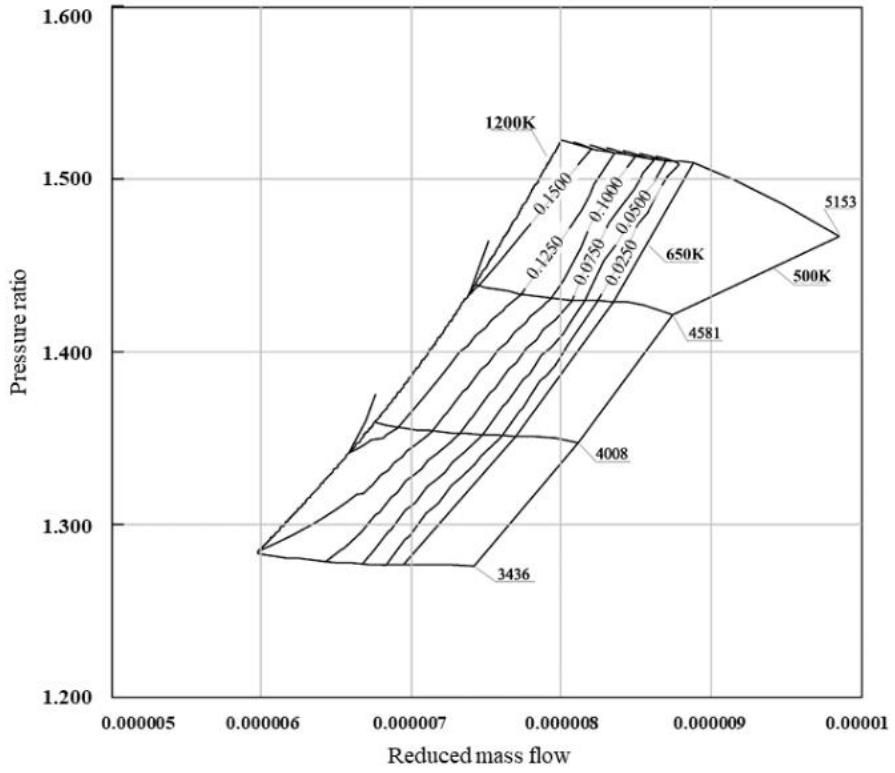

Fig. 10 Performance map, main compressor bypass valve 100% open

Fig. 9 shows system performance map when the compressor bypass valve is partially open (25%). In this scenario overall system efficiency drops and varies from 5 to 30% within the operation range, peaking at highest TIT and highest rotational speed. Fig. 10 shows system performance map when the main compressor bypass valve is fully open. In this scenario overall system efficiency drops significantly and varies from 0 to 15% within the operation range, peaking at highest TIT and highest rotational speed. To avoid drop of efficiency into negative values Turbine Inlet Temperature is assumed to be higher then 650 K.

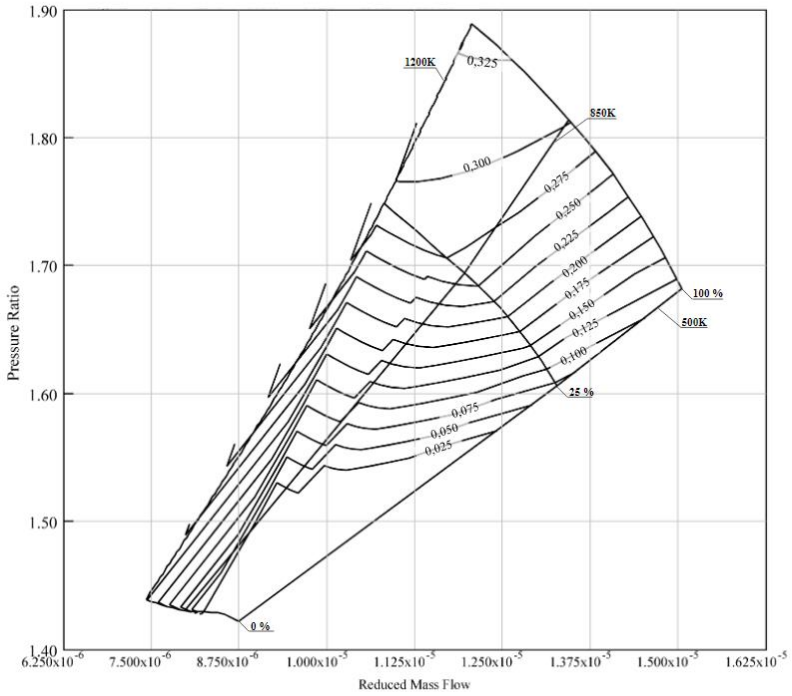

Fig. 11 Grid mode (constant speed) system performance map

During grid mode operation when small units considered, rotational speed of the power plant is maintained by the grid frequency. System power control can be exercised by varying TIT or the main compressor bypass valve opening, but it does not affect rotational speed. Fig. 11 shows an example of a pressure ratio vs reduced mass flow system performance map for grid mode and constant speed. On the map, the vertical lines represent turbine inlet temperature, whereas the horizontal lines represent main compressor bypass valve opening and separated curves show total system efficiency. The map can be used in the controller to determine the main compressor bypass valve position for a given target power or efficiency at given TIT.

On the other hand, during island mode operation, the rotational speed is not maintained by the grid and has to be controlled. System power control is also exercised by varying TIT and the main compressor bypass valve opening. Those two variables are, however, strongly connected and have a major influence on system rotational speed. Knowing these dependencies is important when developing a proper controller.

TIT control can be used to change power output and maintain high system efficiency. The limitation of this strategy is the range of TIT that can be achieved. The main compressor bypass valve control has a significant efficiency penalty, as shown in Fig 10. By combining those two parameters control delivers efficient power regulation and rapid reaction to load changes.

CONCLUSIONS

The presented simulation results indicate that the analyzed sCO2 recompression cycle possesses high operational and control flexibility while at the same time maintaining stable thermal efficiency. The system can operate across a very wide range of parameter change.

Each curve of constant mass flow has two limitations: on both its right-hand side and left-hand side caused by the bypass valve positions and Turbine Inlet Temperatures, respectively. On the right-hand side, the limitation of the bypass valve position goes to unity whereas on the left-hand side the limitation of the TIT exceeds 1200 K.

It can be seen that the system attains slightly higher efficiencies and power outputs when lowering the rational shaft speed than at its design point. This is caused in part by the type of compressor map taken into account, but it would appear that this fact is not decisive. The compressor operation area is distant from the surge limit. This means that the compressor does not limit system operation.

In general, it should be underlined that in the case of a system with an sCO2 recompression cycle there is a possibility of changing the system power output by changing not only the bypass valve position but also the TIT at variable rotational speeds of the compressor-turbine unit. This is accompanied by different system efficiencies. So, there is a need to formulate an appropriate control concept (logic) and approach for technical realization.

REFERENCES

Saber Sadeghi, Ighball Baniasad Askari. Prefeasibility techno-economic assessment of a hybrid power plant with photovoltaic fuel cell and Compressed Air Energy Storage (CAES). Energy 168, 409–424 Elsevier BV, 2019.

Grazia Leonzio. State of art and perspectives about the production of methanol dimethyl ether and syngas by carbon dioxide hydrogenation. Journal of CO2 Utilization 27, 326–354 Elsevier BV, 2018.

Luís Amaral, Justyna Minkiewicz, Biljana Šljukić, Diogo M. F. Santos, César A. C. Sequeira, Milan Vraneš, Slobodan Gadžurić. Toward Tailoring of Electrolyte Additives for Efficient Alkaline Water Electrolysis: Salicylate-Based Ionic Liquids. ACS Applied Energy Materials 1, 4731–4742 American Chemical Society (ACS), 2018.

L. Barelli, G. Bidini, G. Cinti. Air variation in SOE: Stack experimental study. International Journal of Hydrogen Energy 43, 11655–11662 Elsevier BV, 2018.

Yangyang Guo, Tianmin Guo, Shijie Zhou, Yujie Wu, Hui Chen, Xuemei Ou, Yihan Ling. Characterization of Sr2Fe1.5Mo0.5O6-\(\updelta\) -Gd0.1Ce0.9O1.95 symmetrical electrode for reversible solid oxide cells. Ceramics International 45, 10969–10975 Elsevier BV, 2019.

Xuetao Xing, Jin Lin, Yonghua Song, Qiang Hu, You Zhou, Shujun Mu. Optimization of hydrogen yield of a high-temperature electrolysis system with coordinated temperature and feed factors at various loading conditions: A model-based study. Applied Energy 232, 368–385 Elsevier BV, 2018.

José G. García Clúa, Ricardo J. Mantz, Hernán De Battista. Optimal sizing of a grid-assisted wind-hydrogen system. Energy Conversion and Management 166, 402–408 Elsevier BV, 2018.

Mayra Recalde, Theo Woudstra, P.V. Aravind. Renewed sanitation technology: A highly efficient faecal-sludge gasificationsolid oxide fuel cell power plant. Applied Energy 222, 515–529 Elsevier BV, 2018.

Juan Pedro Perez-Trujillo, Francisco Elizalde-Blancas, Massimiliano Della Pietra, Stephen J. McPhail. A numerical and experimental comparison of a single reversible molten carbonate cell operating in fuel cell mode and electrolysis mode. Applied Energy 226, 1037–1055 Elsevier BV, 2018.

Zhuolin Ye, Xin Zhang, Wangyang Li, Guozhen Su, Jincan Chen. Optimum operation states and parametric selection criteria of a high temperature fuel cell-thermoradiative cell system. Energy Conversion and Management 173, 470–475 Elsevier BV, 2018.

Dibyendu Roy, Samiran Samanta, Sudip Ghosh. Energetic exergetic and economic (3E) investigation of biomass gasification-based power generation system employing molten carbonate fuel cell (MCFC), indirectly heated air turbine and an organic Rankine cycle. Journal of the Brazilian Society of Mechanical Sciences and Engineering 41 Springer Nature, 2019.

M. Boroumand, A. M. Tousi. Using inlet guide vane to improve load following ability of solid oxide fuel cell and gas turbine hybrid cycle. Journal of Mechanical Science and Technology 33, 1897–1905 Springer Nature, 2019.

Xiaojing Lv, Xiaoyi Ding, Yiwu Weng. Performance Analysis of an Intermediate-Temperature-SOFC/Gas Turbine Hybrid System Using Gasified Biomass Fuel in Different Operating Modes. Journal of Engineering for Gas Turbines and Power 141, 011501 ASME International, 2018.

Mohammad Marefati, Mehdi Mehrpooya, Mohammad Behshad Shafii. A hybrid molten carbonate fuel cell and parabolic trough solar collector combined heating and power plant with carbon dioxide capturing process. Energy Conversion and Management 183, 193–209 Elsevier BV, 2019.

Janusz Badur, Marcin Lemański, Tomasz Kowalczyk, Paweł Ziółkowski, Sebastian Kornet. Zero-dimensional robust model of an SOFC with internal reforming for hybrid energy cycles. Energy 158, 128–138 Elsevier BV, 2018.

Chen Chen, Leilei Zhao, Adrienne S. Lavine. Feasibility of using ammonia-based thermochemical energy storage to produce high-temperature steam or sCO2. Solar Energy 176, 638–647 Elsevier BV, 2018.

D. Sánchez, R. Chacartegui, J.M. Muñoz de Escalona, A. Muñoz, T. Sánchez. Performance analysis of a MCFC & supercritical carbon dioxide hybrid cycle under part load operation. International Journal of Hydrogen Energy 36, 10327–10336 Elsevier BV, 2011.

John J. Dyreby, Sanford A. Klein, Gregory F. Nellis, Douglas T. Reindl. Modeling Off-Design and Part-Load Performance of Supercritical Carbon Dioxide Power Cycles. In Volume 8: Supercritical CO2 Power Cycles\(\mathsemicolon\) Wind Energy\(\mathsemicolon\) Honors and Awards. ASME, 2013.

John J Dyreby, Sanford A Klein, Gregory F Nellis, Douglas T Reindl. Modeling off-design operation of a supercritical carbon dioxide Brayton cycle. 24–25 In Proceedings of Supercritical CO2 Power Cycle Symposium, Boulder, Colorado May. (2011).

John Dyreby, Sanford Klein, Gregory Nellis, Douglas Reindl. Design Considerations for Supercritical Carbon Dioxide Brayton Cycles with Recompression. Journal of Engineering for Gas Turbines and Power 136, 101701 ASME International, 2014.

John Vega, Chandrashekhar Sonwane, Tony Eastland. Supercritical CO2 turbomachinery configuration and controls for a zero-emission coal fired power plant: system off design & control of system transients. 9–10 In 4th International Symposium on Supercritical CO2 Power Cycles, Pittsburgh, PA, September. (2014).

A Tse Louis, Ty Neises. Analysis and Optimization for Off-Design performance of the recompression s-CO2 cycles for high temperature CSP applications. In The 5th International Symposium-Supercritical CO2 Power Cycles. (2016).

Kevin Hoopes, David Sánchez, Francesco Crespi. A New Method for Modelling Off-Design Performance of sCO 2 Heat Exchangers Without Specifying Detailed Geometry. 28–31 In Fifth Supercritical CO 2 Power Cycles Symposium, San Antonio, TX, Mar. (2016).

Jinsu Kwon, Jeong Ik Lee. Development of accelerated PCHE off-design performance model for optimizing power system control strategies in S-CO2 system. In 6th International Supercritical Symposium CO2 Power Cycles Symposium. (2018).

Steven A Wright, Chal Davidson, Craig Husa. Off-Design Performance Modeling Results for a Supercritical CO2 Waste Heat Recovery Power System.

Di Zhang, Yuqi Wang, Yonghui Xie. Investigation into Off-Design Performance of a S-CO2 Turbine Based on Concentrated Solar Power. Energies 11, 3014 MDPI AG, 2018.

Firman Bagja Juangsa, Lukman Adi Prananto, Zahrul Mufrodi, Arief Budiman, Takuya Oda, Muhammad Aziz. Highly energy-efficient combination of dehydrogenation of methylcyclohexane and hydrogen-based power generation. Applied Energy 226, 31–38 Elsevier BV, 2018.

M.L. Ferrari, M. Pascenti, A.F. Massardo. Validated ejector model for hybrid system applications. Energy 162, 1106–1114 Elsevier BV, 2018.

Kun Wang, Ya-Ling He. Thermodynamic analysis and optimization of a molten salt solar power tower integrated with a recompression supercritical CO 2 Brayton cycle based on integrated modeling. Energy Conversion and Management 135, 336–350 Elsevier BV, 2017.

Minh Tri Luu, Dia Milani, Robbie McNaughton, Ali Abbas. Dynamic modelling and start-up operation of a solar-assisted recompression supercritical CO 2 Brayton power cycle. Applied Energy 199, 247–263 Elsevier BV, 2017.

Minh Tri Luu, Dia Milani, Robbie McNaughton, Ali Abbas. Advanced control strategies for dynamic operation of a solar-assisted recompression supercritical CO 2 Brayton power cycle. Applied Thermal Engineering 136, 682–700 Elsevier BV, 2018.

Dia Milani, Minh Tri Luu, Robbie McNaughton, Ali Abbas. A comparative study of solar heliostat assisted supercritical CO2 recompression Brayton cycles: Dynamic modelling and control strategies. The Journal of Supercritical Fluids 120, 113–124 Elsevier BV, 2017.

Xiaohe Wang, Qibin Liu, Jing Lei, Wei Han, Hongguang Jin. Investigation of thermodynamic performances for two-stage recompression supercritical CO 2 Brayton cycle with high temperature thermal energy storage system. Energy Conversion and Management 165, 477–487 Elsevier BV, 2018.

M.A. Reyes-Belmonte, A. Sebastián, M. Romero, J. González-Aguilar. Optimization of a recompression supercritical carbon dioxide cycle for an innovative central receiver solar power plant. Energy 112, 17–27 Elsevier BV, 2016.

L.A. de Araujo Passos, S.L. de Abreu, A.K. da Silva. Time-dependent behavior of a recompression cycle with direct CO 2 heating through a parabolic collector array. Applied Thermal Engineering 140, 593–603 Elsevier BV, 2018.

Maimoon. Atif, Fahad A. Al-Sulaiman. Energy and exergy analyses of solar tower power plant driven supercritical carbon dioxide recompression cycles for six different locations. Renewable and Sustainable Energy Reviews 68, 153–167 Elsevier BV, 2017.

Shubham Banik, Satyaki Ray, Sudipta De. Thermodynamic modelling of a recompression CO2 power cycle for low temperature waste heat recovery. Applied Thermal Engineering 107, 441–452 Elsevier BV, 2016.

Shengya Hou, Yuandan Wu, Yaodong Zhou, Lijun Yu. Performance analysis of the combined

supercritical CO 2 recompression and regenerative cycle used in waste heat recovery of marine gas turbine. Energy Conversion and Management 151, 73–85 Elsevier BV, 2017.

Alberto de la Calle, Alicia Bayon, Yen Chean Soo Too. Impact of ambient temperature on supercritical CO 2 recompression Brayton cycle in arid locations: Finding the optimal design conditions. Energy 153, 1016–1027 Elsevier BV, 2018.

Xurong Wang, Yiping Dai. Exergoeconomic analysis of utilizing the transcritical CO2 cycle and the ORC for a recompression supercritical CO2 cycle waste heat recovery: A comparative study. Applied Energy 170, 193–207 Elsevier BV, 2016.

Shengya Hou, Yaodong Zhou, Lijun Yu, Fengyuan Zhang, Sheng Cao, Yuandan Wu. Optimization of a novel cogeneration system including a gas turbine a supercritical CO 2 recompression cycle, a steam power cycle and an organic Rankine cycle. Energy Conversion and Management 172, 457–471 Elsevier BV, 2018.

F.A. Al-Sulaiman. On the auxiliary boiler sizing assessment for solar driven supercritical CO 2 double recompression Brayton cycles. Applied Energy 183, 408–418 Elsevier BV, 2016.

Q.H. Deng, D. Wang, H. Zhao, W.T. Huang, S. Shao, Z.P. Feng. Study on performances of supercritical CO 2 recompression Brayton cycles with multi-objective optimization. Applied Thermal Engineering 114, 1335–1342 Elsevier BV, 2017.

Chuang Wu, Shun-sen Wang, Xue-jia Feng, Jun Li. Energy exergy and exergoeconomic analyses of a combined supercritical CO 2 recompression Brayton/absorption refrigeration cycle. Energy Conversion and Management 148, 360–377 Elsevier BV, 2017.

Chuang Wu, Shun-sen Wang, Jun Li. Exergoeconomic analysis and optimization of a combined supercritical carbon dioxide recompression Brayton/organic flash cycle for nuclear power plants. Energy Conversion and Management 171, 936–952 Elsevier BV, 2018.

Woo Seok Jeong, Jeong Ik Lee, Yong Hoon Jeong. Potential improvements of supercritical recompression CO2 Brayton cycle by mixing other gases for power conversion system of a SFR. Nuclear Engineering and Design 241, 2128–2137 Elsevier BV, 2011.

Ata D. Akbari, Seyed M.S. Mahmoudi. Thermoeconomic analysis & optimization of the combined supercritical CO 2 (carbon dioxide) recompression Brayton/organic Rankine cycle. Energy 78, 501–512 Elsevier BV, 2014.

J. Floyd, N. Alpy, A. Moisseytsev, D. Haubensack, G. Rodriguez, J. Sienicki, G. Avakian. A numerical investigation of the sCO2 recompression cycle off-design behaviour coupled to a sodium cooled fast reactor, for seasonal variation in the heat sink temperature. Nuclear Engineering and Design 260, 78–92 Elsevier BV, 2013.

T. Conboy, J. Pasch, D. Fleming. Control of a Supercritical CO2Recompression Brayton Cycle Demonstration Loop. In Volume 8: Supercritical CO2 Power Cycles\(\mathsemicolon\) Wind Energy\(\mathsemicolon\) Honors and Awards. ASME, 2013.

Marcin Plis, Henryk Rusinowski. A mathematical model of an existing gas-steam combined heat and power plant for thermal diagnostic systems. Energy 156, 606–619 Elsevier BV, 2018.

G. Botta, M. Romeo, A. Fernandes, S. Trabucchi, P.V. Aravind. Dynamic modeling of reversible solid oxide cell stack and control strategy development. Energy Conversion and Management 185, 636–653 Elsevier BV, 2019.

Rui Ma, Chen Liu, Elena Breaz, Pascal Briois, Fei Gao. Numerical stiffness study of multi-physical solid oxide fuel cell model for real-time simulation applications. Applied Energy 226, 570–581 Elsevier BV, 2018.

Pravin P. S., Ravindra Gudi, Sharad Bhartiya. Dynamic Modeling and Control of an Integrated Reformer-Membrane-Fuel Cell System. Processes 6, 169 MDPI AG, 2018.

Osamah Siddiqui, Ibrahim Dincer. A Review on Fuel Cell-Based Locomotive Powering Options for Sustainable Transportation. Arabian Journal for Science and Engineering 44, 677–693 Springer Nature, 2018.

Yan Xia, Jianxiao Zou, Wenxu Yan, Huayin Li. Adaptive Tracking Constrained Controller Design for Solid Oxide Fuel Cells Based on a Wiener-Type Neural Network. Applied Sciences 8, 1758 MDPI AG, 2018.

M.M Shah. A general correlation for heat transfer during film condensation inside pipes. International Journal of heat and mass transfer 22(4), pp.547-556 (1979).

ACKNOWLEDGEMENTS

This work is financed by the National Science Center, Poland, 2015/19/D/ST8/02780.